

1 **Comparative Population Genomics of Bread Wheat (*Triticum***
2 ***aestivum*) Reveals Its Cultivation and Breeding History in China**

3 Haofeng Chen^{1,2,7,8}, Chengzhi Jiao^{3,8}, Ying Wang^{1,8}, Yuange Wang^{2,8}, Caihuan Tian²,
4 Haopeng Yu^{1,2,4}, Jing Wang², Xiangfeng Wang⁵, Fei Lu^{1,6}, Xiangdong Fu^{1,6},
5 Yongbiao Xue^{1,6}, Wenkai Jiang³, Hongqing Ling^{1,6}, Hongfeng Lu^{3*}, Yuling Jiao^{1,2*}

6 ¹College of Life Sciences, University of Chinese Academy of Sciences, Beijing 100049,
7 China.

8 ²State Key Laboratory of Plant Genomics, Institute of Genetics and Developmental Biology,
9 Chinese Academy of Sciences, Beijing 100101, China.

10 ³Novogene Bioinformatics Institute, Beijing 100083, China.

11 ⁴West China Biomedical Big Data Center, West China Hospital/West China School of
12 Medicine, and Medical Big Data Center, Sichuan University, Chengdu 610041, China.

13 ⁵Department of Crop Genomics and Bioinformatics, College of Agronomy and
14 Biotechnology, National Maize Improvement Center of China, China Agricultural University,
15 Beijing 100193, China.

16 ⁶State Key Laboratory of Plant Cell and Chromosome Engineering, Institute of Genetics and
17 Developmental Biology, Chinese Academy of Sciences, Beijing 100101, China.

18 ⁷Present address: National Research Institute for Family Planning, Beijing, 100081, China

19 ⁸These authors contributed equally to this work.

20 *Correspondence to: yljiao@genetics.ac.cn (Y.J.); luhongfeng@novogene.cn (H.Lu)

21

22 **Abstract**

23 **The evolution of bread wheat (*Triticum aestivum*) is distinctive in that**
24 **domestication, natural hybridization, and allopolyploid speciation have all had**
25 **significant effects on the diversification of its genome. Wheat was spread around**
26 **the world by humans and has been cultivated in China for ~4,600 years. Here,**
27 **we report a comprehensive assessment of the evolution of wheat based on the**
28 **genome-wide resequencing of 120 representative landraces and elite wheat**
29 **accessions from China and other representative regions. We found substantially**
30 **higher genetic diversity in the A and B subgenomes than in the D subgenome.**

31 **Notably, the A and B subgenomes of the modern Chinese elite cultivars were**
32 **mainly derived from European landraces, while Chinese landraces had a greater**
33 **contribution to their D subgenomes. The duplicated copies of homoeologous**
34 **genes from the A, B, and D subgenomes were commonly found to be under**
35 **different levels of selection. Our genome-wide assessment of the genetic changes**
36 **associated with wheat breeding in China provides new strategies and practical**
37 **targets for future breeding.**

38

39 **Main**

40 Bread wheat (*Triticum aestivum*) differs from other major grain crops, such as maize
41 (*Zea mays*), rice (*Oryza sativa*), and barley (*Hordeum vulgare*), by having an
42 allohexaploid genome with six sets of chromosomes, two sets each from three closely
43 related ancestral species that formed the A, B, and D subgenomes. Archaeological and
44 genetic evidence indicated that wheat underwent two polyploidization events during
45 its domestication. The first occurred ~0.82 million years ago between two diploid
46 species, *T. urartu* (AA) and an unknown close relative of *Aegilops speltoides* (SS),
47 which produced the allotetraploid *T. turgidum* (AABB). The second polyploidization
48 occurred during cultivation around 8,000–10,000 years ago, when *T. turgidum*
49 crossed with another diploid grass, *Ae. tauschii* (DD), to form the ancestral bread
50 wheat (*T. aestivum*, AABBDD)¹⁻⁴. In addition, a recent genome analysis suggested
51 that *Ae. tauschii* originated from a more ancient homoploid hybridization event
52 between the A and B lineage ancestors⁵. The A, B, and D subgenomes comprise the
53 ~17-Gb allohexaploid bread wheat genome. Enormous genome sequencing efforts
54 have resulted in the recent publication of a reference genome sequence for wheat^{4,6-9},
55 which has greatly enhanced our understanding of the genome of this vital crop.

56 After its evolution in the Middle East and Mediterranean regions, bread wheat
57 gradually spread to the rest of the world and was domesticated for human use¹⁰. China

58 has been cultivating bread wheat for ~4,600 years^{11,12}, and has been the largest wheat-
59 producing country for more than two decades. Wheat has been under continuous
60 artificial selection in the diverse ecological zones of China for thousands of years^{11,13};
61 thus, the domestication and breeding of bread wheat in this country provides unique
62 evolutionary insights into how its genome diversity was used and altered to meet the
63 changing needs of the human population.

64 Recent advances in wheat genome sequencing have made pangenome studies
65 possible^{14,15}. To understand wheat genome diversity and evolution, we resequenced
66 120 landraces and elite bread wheat accessions at above a ten-fold coverage, and
67 employed the resequencing data to unravel the genealogical history of wheat
68 domestication. We identified the hybrid origins of various wheat cultivars and
69 landraces, especially those cultivated in China. Using these data, we began to
70 elucidate the genomic signatures that underlie human selection during the history of
71 wheat breeding.

72

73 **Results**

74 **Characterization of molecular diversity**

75 We selected 120 wheat accessions for our study, including 95 landraces and 25
76 cultivars. The 60 Chinese accessions are representative ones of a Chinese mini core
77 collection (Supplementary Fig. 1a and b), which covers the widest genome diversity
78 of 23,090 Chinese landraces and cultivars¹⁶. The other accessions were selected based
79 on genotyping-by-sequencing results of 326 representative species collected
80 worldwide (Supplementary Fig. 1c). Notably, we selected 16 accessions from the
81 regions of the Fertile Crescent where wheat was first cultivated. Thus, the
82 resequenced accessions represent the widest genome diversity of both Chinese and
83 worldwide wheat populations. The geographic distributions of these accessions
84 included East Asia (China and Japan), West Asia, Central and South Asia, Europe,
85 and America (Fig. 1a and Supplementary Table 1).

86 A total of 21,676 Tb of sequence data was generated from the 120 accessions
87 using Illumina paired-end short-read technology, with an average read depth of
88 11.04× for each individual (Supplementary Table 2). The reads were mapped against
89 the IWGSC RefSeq v1.0 assembly of the wheat genome⁹ to identify genomic variants,
90 yielding a ~90% coverage of the genome by at least four reads for each wheat
91 accession. We detected a total of 70,172,600 single-nucleotide polymorphisms
92 (SNPs) using the SAMtools software¹⁷, with an average density of 4.82 SNPs per kb.
93 Most of these SNPs were located in intergenic regions (94.76%), with only 1.43%
94 located in exonic regions (Table 1 and Supplementary Fig. 2). Of the SNPs located in
95 exonic regions, 36.62% were synonymous and 54.80% were non-synonymous, with a
96 non-synonymous/synonymous (N/S) ratio of 1.5. This N/S ratio is higher than was
97 previously reported for other plants such as sorghum (*Sorghum bicolor*; N/S ratio =
98 1.0)¹⁸, rice (N/S ratio = 1.2)¹⁹, soybean (*Glycine max*; N/S ratio = 1.47)²⁰, and
99 *Arabidopsis thaliana* (N/S ratio = 0.83)²¹.

100 We found that the A and B subgenomes harbor similar numbers of SNPs, with
101 the B subgenome (~32.95 M, 6.36 SNPs per kb) containing slightly more than the A
102 subgenome (~28.72 M, 5.82 SNPs per kb). By contrast, the D subgenome included
103 only ~7.91 M SNPs and had the lowest SNP density (2.00 SNPs per kb) (Table 1, Fig.
104 1c). A previous finding showed that low numbers of polymorphic loci in the D
105 subgenome may be a specific attribute of wheat, not of the D subgenome progenitor
106 *Ae. tauschii*²². In all three wheat subgenomes, the majority of SNPs were located in
107 intergenic regions, and non-synonymous SNPs were more common than synonymous
108 SNPs (the N/S ratios of A, B, and D subgenomes were 1.56, 1.59, and 1.28,
109 respectively; Table 1). In the wheat reference genome (IWGSC RefSeq Annotation
110 v1.0), the gene models were classified into high-confidence (HC) and low-confidence
111 (LC) genes based on their predicted sequence homology to gene products in the
112 public database. In the coding regions, 47.78% of the SNPs were located in HC genes.
113 These SNPs also had N/S ratios greater than 1 (Supplementary Table 3).

114 To measure the degree of polymorphism in the wheat genome, we measured
115 the nucleotide diversity parameters π and Watterson's θ . The overall wheat genomic
116 nucleotide diversity (π) was 1.05×10^{-3} , and Watterson's θ was 0.84×10^{-3} , which is
117 consistent with a previous report ($\pi = 0.8 \times 10^{-3}$)²³. The nucleotide diversity parameter
118 for wheat was lower than for other major crops, including maize ($\pi = 6.6 \times 10^{-3}$)²⁴,
119 rice ($\pi = 2.29 \times 10^{-3}$)²⁵, and sorghum ($\pi = 2.4 \times 10^{-3}$)²⁶. The π value of the cultivars
120 (0.92×10^{-3}) was only slightly lower than that of the landraces (1.04×10^{-3}).
121 Similarly, the Watterson's θ value for the cultivars (0.84×10^{-3}) was slightly lower
122 than that of the landraces (0.87×10^{-3}). The mean fixation index value (F_{ST}) between
123 the cultivars and landraces was 0.03, suggesting limited population divergence
124 between the cultivars and landraces.

125 We then separated the data into the A, B, and D subgenomes to understand
126 their individual genetic diversities (Fig. 1b and Supplementary Table 4). In the
127 individual A, B, and D subgenomes, the nucleotide diversity parameters π and
128 Watterson's θ were similar between the landraces and cultivars, indicating that the
129 modern wheat cultivars retained most of the genetic diversity of the landraces during
130 their domestication. The π and Watterson's θ values each demonstrated that the A and
131 B subgenomes had similar nucleotide diversities, while the D subgenome had only
132 ~20% of the genetic diversity of the A or B subgenomes (Fig. 1c), consistent with a
133 previous report¹⁵. The heterozygous rates of all accessions were low (average:
134 0.1655%), reflecting the lack of cross-pollination, consistent with the cleistogamy of
135 wheat flowers. Among the three subgenomes, the D subgenome had a substantially
136 lower heterozygous rate than the A and B subgenomes (Supplementary Table 5),
137 consistent with its lower genetic diversity.

138 Tajima's D was calculated to assess whether the observed nucleotide
139 diversities showed evidence of deviation from neutrality. Some regions were
140 significantly different from zero, which indicates that they may be under sweep

141 selection (Fig. 1b). Of these, the D values from the A and B subgenomes were mostly
142 positive, whereas those of the D subgenome were generally negative (Fig. 1c and
143 Supplementary Table 4). Negative Tajima's D values indicate the presence of low-
144 frequency SNPs in the D subgenome, while the positive Tajima's D values indicate a
145 predominance of intermediate-frequency SNPs in the A and B subgenomes. The
146 minor allele frequency (MAF) in the A, B, and D subgenomes significantly correlated
147 with the Tajima's D values (Supplementary Table 6). Because the three subgenomes
148 were expected to have experienced a similar evolution history in the allohexaploid
149 wheat after the second polyploidization event, the dramatic difference between D
150 subgenome and the A and B subgenomes indicates an asymmetric selection history
151 during domestication. Gene flow to bread wheat from wild and/or cultivated
152 tetraploid *T. turgidum* (AABB genome) is likely common, as suggested by the
153 identification of hybrid swarms between wild emmer wheat (*T. turgidum* subsp.
154 *dicoccoides*) and bread wheat^{27,28}. By contrast, the barrier to gene flow from *Ae.*
155 *tauschii* (DD genome) to bread wheat is much more difficult to overcome.
156 Nevertheless, this difference may also contribute to the variations in the evolution
157 rates between the subgenomes.

158 **Population structure**

159 To explore the phylogenetic relationships among the 120 wheat accessions, we
160 constructed a phylogenetic tree using the neighbor-joining algorithm, based on the
161 pairwise genetic distances between each accession determined using the SNP
162 information. The phylogenetic analysis clustered the wheat accessions into two
163 groups. Group 1 incorporated most of the European landraces, the West Asian
164 landraces (marked as "Origin"), a few South and Central Asian landraces, and the
165 majority of the East Asian cultivars (Fig. 2a). In group 2, most of the East Asian
166 landraces were clustered together alongside some of the West Asian landraces and the
167 majority of the South and Central Asian landraces (Fig. 2a). These two clearly defined
168 groups were further strengthened by the results of a principal component analysis

169 (PCA) and the Bayesian model-based clustering method (Fig. 2b). At $K = 2$, the group
170 1 accessions formed one cluster, while those of group 2 formed the other cluster. At
171 the optimal presumed number of ancestral populations ($K = 3$), the landraces near the
172 origin site (West, South, and Central Asian accessions) were separated from the main
173 groups. At $K = 4$, the West Asian and South and Central Asian accessions were
174 clearly divided. At $K = 5$, we obtained more refined clusters associated with the
175 geographic distributions (Fig. 2c and Supplementary Fig. 5). These findings were
176 consistent with the geographic documentation of wheat: from its domestication in the
177 Fertile Crescent, bread wheat was transported west to Europe and America, and east
178 to South and Central Asia and finally to East Asia via separate routes (Supplementary
179 Fig. 4)¹⁰. Our phylogenetic analysis, PCA, and clustering approaches revealed that
180 only a few Chinese cultivars are closely related to the Chinese landraces (Fig. 2a and
181 B). The population structure revealed that the Chinese cultivars are clearly related to
182 the European (and American) landraces when $K = 2-5$ (Fig. 2c). It is therefore evident
183 that the Chinese landraces contributed a minor portion of the genetic diversity of the
184 Chinese cultivars.

185 To understand whether different diploid ancestors contributed similar amounts
186 of genetic diversity to the subgenomes, we further analyzed the population structure
187 of each subgenome separately. The A and B subgenome population structures
188 confirmed the evolutionary patterns observed for the whole genome (Supplementary
189 Figs. 6 and 7). In contrast, the D subgenomes of most Chinese cultivars were closely
190 related to the Chinese landraces in the phylogenetic tree analysis, which was further
191 supported by the results of the PCA and genetic structure analysis (Supplementary
192 Fig. 9). Taken together, the A and B subgenomes of the Chinese cultivars may mainly
193 come from European landraces and cultivars with a genetic admixture of Chinese
194 landraces, whereas the D subgenome contains more of a contribution from the
195 Chinese landraces with a lesser admixture of European landraces.

196 To investigate the differences in genetic diversity between the three
197 populations (Chinese cultivars, Chinese landraces, and European landraces), we
198 calculated the nucleotide diversities (π) and found no significant difference among the
199 three populations. The diversity of Chinese cultivars was slightly higher than that of
200 the Chinese landraces, but slightly lower than that of the European landraces (Fig.
201 2d). We calculated the F_{ST} values to investigate the population divergences, which
202 revealed that the divergence between the Chinese cultivars and European landraces
203 ($F_{ST} = 0.04$) was smaller than the divergence of the Chinese cultivars and Chinese
204 landraces ($F_{ST} = 0.07$). This analysis indicated a small population divergence (Fig.
205 2d).

206 We further analyzed the linkage disequilibrium (LD) of the three populations.
207 The mean r^2 between 0 and 1000 kb from the three populations was greater than 0.3,
208 suggesting that wheat has a longer LD decay than cultivated rice (123 kb for *indica*
209 varieties) and cultivated maize (30 kb)^{29,30}. The mean r^2 between 0 and 1000 kb of the
210 D subgenome decreased more rapidly than for the A and B subgenomes, suggesting a
211 lower level of selection on the D subgenome (Fig. 2e). The extent of LD in the A, B,
212 and D subgenomes differed between the Chinese cultivars, Chinese landraces, and
213 European landraces. For the A subgenome, the LD decay of the Chinese landraces
214 was slightly higher than that of the European landraces, and significantly higher than
215 that of the Chinese cultivars. For the B subgenome, the Chinese landraces also had the
216 highest LD levels, with the Chinese cultivars and European landraces displaying
217 similar levels of LD decay. In the D subgenome however, the LD decay was similar
218 for all three populations. Different chromosomes had specific patterns of LD
219 (Supplementary Fig. 3), which may be correlated with differences in heterochromatin
220 levels³¹ and selection pressure.

221 **Introgressions from Chinese landraces and European varieties in the Chinese**
222 **cultivars**

223 We used a TreeMix analysis to infer ancient gene flows. A maximum-likelihood
224 (ML) tree without migration events grouped the wheat accessions into seven clusters,
225 which were similar to the above population structure patterns. Furthermore, we
226 detected strong migration events in three clusters, namely the Chinese cultivars,
227 Chinese landraces, and European cultivars. There were strong gene flows from the
228 Chinese landraces to the Chinese cultivars, and from the European landraces to the
229 European cultivars (Supplementary Fig. 6a and b). We next individually analyzed the
230 three subgenomes. The ML trees for the A and B subgenomes of the accessions had
231 similar topological structures to the ML tree using the whole genomes (Fig. 3a). We
232 also found strong gene flows from the Chinese landraces to the Chinese cultivars and
233 from the ancient western landraces to the European landraces in both the A and B
234 subgenomes (Fig. 3a). When the D subgenome was considered, the accessions formed
235 a different ML tree structure, with Chinese landraces grouped with Chinese cultivars,
236 and clear gene flows from the European cultivars to the Chinese cultivars, and from
237 the South and Central Asian landraces to the European landraces (Fig. 3a).

238 To further elucidate the contributions from the European varieties and Chinese
239 landraces to the Chinese cultivars, we used an identity score (IS) analysis³² to scan
240 each chromosome. The IS analyses for the three groups (European varieties, Chinese
241 landraces, and Chinese cultivars) revealed that the Chinese landraces had more
242 similarity to the reference genome (Chinese Spring, a Chinese landrace) than the
243 European and Chinese cultivars, while the Chinese cultivars were more similar to the
244 European varieties than the Chinese landraces (Fig. 3b). Consistent with the results of
245 the population structure analysis, the IS heatmap showed that the European varieties
246 contributed more to the Chinese cultivars than did the Chinese landraces
247 (Supplementary Fig. 10). More differences were detected between the Chinese
248 landraces and the Chinese cultivars than between the European varieties and the
249 Chinese cultivars when using IS values less than 0.0025 as the threshold (Fig. 3c).
250 Specifically, 280,299 regions were detected, spanning 5.61 Gb (39.28% of the

251 genomes), in which the Chinese cultivars and European varieties were more similar
252 than the Chinese cultivars and Chinese landraces, while only 106,453 regions,
253 spanning 2.13 Gb (14.92% of the genomes) were identified in which Chinese
254 cultivars and Chinese landraces were more similar (Fig. 3d). Within most
255 chromosomes, we observed similar patterns of homology, although there were clear
256 variations (Supplementary Fig. 11, Supplementary Table 7a).

257 We were particularly interested in the many exceptionally large dispersed
258 introgression regions identified in the genomes of the wheat population. Between the
259 Chinese landraces and the Chinese cultivars, the introgression regions are mainly
260 located in the A and B subgenomes, while those between the European varieties and
261 the Chinese cultivars were mainly located in the D subgenome. These introgression
262 regions usually show higher heterozygosity, low recombination rates, and long-range
263 LD²⁷; for example, an 8-Mb region in chromosome 5D of the Chinese cultivars is
264 enriched with SNPs from the European varieties (Fig. 3e). Within this region, the
265 Chinese cultivars are highly heterozygous and have low recombination rates, as well
266 as a significantly higher LD level (Fig. 3e). We focused on the mutation sites within
267 this candidate introgression region, which covers 346 genes (Supplementary Table
268 7b). Using a Kyoto Encyclopedia of Genes and Genomes (KEGG) analysis, we
269 observed a significant enrichment of genes involved in pathways related to
270 photosynthesis within this region (Supplementary Table 7d), including genes involved
271 in photosystem I (*TraesCS5D01G552400LC/PSAB*, *TraesCS5D01G552500LC/PSAB*,
272 and *TraesCS5D01G552600LC/PSAB*) and photosystem II
273 (*TraesCS5D01G550000LC/PSBA*, *TraesCS5D01G458100/PSBK*,
274 *TraesCS5D01G458200/PSBI*, *TraesCS5D01G550600LC/PSBA*,
275 *TraesCS5D01G550700LC/PSBC*, *TraesCS5D01G550800LC/PSBC*,
276 *TraesCS5D01G458300/PSBZ*, and *TraesCS5D01G458400/PSBM*). Another 200-Mb
277 region on chromosome 6A of the Chinese cultivars is enriched with SNPs from the
278 Chinese landraces (Fig. 3f). This region also has higher heterozygosity and lower

279 recombination rates within these lines, and shows a significantly higher LD (Fig. 3f).
280 The 2,131 genes within this region (Supplementary Table 7c) were also enriched for
281 oxidative phosphorylation and ribosome pathway functions (Supplementary Table
282 7e). Taken together, our IS analysis revealed the detailed contributions of the
283 European landraces and Chinese landraces to the Chinese cultivars. Importantly, most
284 of these regions are genome-specific, suggesting the functional diversification of the
285 three genomes.

286 **Selective signals during diversification and modern breeding**

287 To identify the genomic regions most affected by selection during wheat
288 diversification and modern breeding in China, we scanned the patterns of genetic
289 variation along the chromosomes on the basis of the 70.12 million SNPs. We
290 calculated the nucleotide diversity ratio ($\theta_{\pi \text{ landrace}}/\theta_{\pi \text{ cultivar}}$) and genetic differentiation
291 (F_{ST}) between the cultivars and landraces. Long stretches of elevated F_{ST} were found
292 along chromosome 4A, which is known to contain structurally rearranged
293 chromosomal regions³³. After excluding these rearranged regions, the top 5% of
294 regions (~14.98 Mb) were considered putative sweep-selected sections, which
295 contained 842 genes (Supplementary Table 8a). A comparison among the
296 subgenomes indicated that selection in the D subgenome is substantially lower than in
297 the A and B subgenomes, as indicated by the lower F_{ST} and nucleotide diversity ratio
298 ($\theta_{\pi \text{ landrace}}/\theta_{\pi \text{ cultivar}}$) for the D subgenome (Fig. 1b). The A subgenome had the most
299 selected regions (Supplementary Table 8b). We also used the XP-EHH³⁴ and XP-
300 CLR³⁵ methods to identify the regions under sweep selection, which respectively led
301 to the identification of 2.65 Mb (948 genes) and 16.63 Mb (2,168 genes) of the
302 putatively selected regions (Supplementary Table 8c and d). The combination of the
303 results from all approaches led to the identification of a total of 3,659 genes, the
304 majority of which were located on the A and B subgenomes (Supplementary Table
305 8f). The selected regions contain many previously reported quantitative trait loci
306 (QTL); for example, one on chromosome 6B and one on chromosome 7D both

307 associated with the length of the uppermost internode length³⁶. Gene Ontology (GO)
308 and KEGG enrichment analyses revealed that the selected regions are enriched in
309 genes with decarboxylating activity and glycine catabolism, suggesting that the
310 carbon metabolic pathways were targeted during modern breeding. Additional
311 pathways, such as selenocompound metabolism, were also under selection
312 (Supplementary Tables 7g and h).

313 The allotetraploid nature of bread wheat raised the question of whether the
314 duplicate copies of the homoeologous genes are all under selection. Using the ordered
315 sets of homoeologous genes, we established the syntenic relationships of the selected
316 targets on the other subgenomes (Fig. 4b). This analysis indicated that some syntenic
317 regions shared the signature of selection; for example, the syntenic regions of
318 chromosomes 6A, 6B, and 6D were all under selection (Fig. 4b, Supplementary Table
319 8i). In the majority of cases however, we could not identify selection signatures in the
320 syntenic regions, suggesting that the homoeologous genes are generally under
321 differing selection pressures and are likely responsible for new functions.

322 To identify the high-confidence sweep-selected regions, we focused on the
323 overlapping regions commonly identified using the three above-mentioned
324 approaches, which contained 48 HC genes (Supplementary Table 8e). Chromosome
325 6B had the strongest selection signal. A sub-region of this selected region contains
326 *TaNPF6.1-6B* (Fig. 4c), an ortholog of the *Arabidopsis* nitrate transporter gene
327 *NRT1.1*^{37,38}. Within the same selected region, we also found *TaNAC24*, the ortholog
328 of a gene that confers heat and drought tolerance in rice³⁹. In a neighboring sub-
329 region, we found strong selection signals for *TaRVE3* (which encodes a putative
330 circadian clock and flowering time regulator)⁴⁰, and *TaHDG2* (encoding a putative
331 stomata and epidermis patterning regulator)⁴¹, suggesting the existence of a selected
332 region regulating multiple traits on chromosome 6B (Fig. 4c). In another selected
333 region on chromosome 3A, we identified *TaHSP101*, which enhances tolerance to salt

334 and desiccation stresses⁴²; *TaPTR7*, the ortholog of a rice NAC transcription factor
335 conferring salt tolerance⁴³; and *TaPRO1*, a component on the actin cytoskeleton
336 potentially related to grain size⁴⁴ (Fig. 4c). The majority of the selected features and
337 genes are currently poorly annotated and warrant further investigation.

338 We analyzed the haplotype frequency of the annotated genes under sweep
339 selection, except *TaPTR7* as it contained no SNPs. In the landraces, the frequencies of
340 the primary haplotypes of all selected genes were lower than in the cultivars (Fig. 4d
341 and 4e). Different periods of wheat breeding history likely had diverse breeding goals.
342 To clarify the changes in the haplotypes of these genes over time, we screened the
343 SNPs of six genes in the selected regions (*TaAGL29*, *TaHDG2*, *TaKNAT6*,
344 *TaMADS21*, *TaRGI5*, and *WSD1-like*) for Chinese cultivars released between the
345 1940s and the 2000s (Supplementary Table 12b). For each gene, the frequency of the
346 favorable haplotype gradually increased over time (Fig. 4f).

347 **Local adaption and related traits**

348 Our phylogenetic analysis showed that landraces from geographically close regions
349 tended to be more genetically similar (Fig. 2). To understand the selection undergone
350 by the genes and corresponding traits of these genotypes during geographic
351 diversification and/or local breeding, we calculated the population differentiation
352 across different geographic groups.

353 The European landraces contributed the majority of the A and B subgenomes
354 of the Chinese cultivars (Supplementary Figs. 7 and 8). We compared these two
355 groups to identify the regions selected during the local adaptation of the Chinese
356 cultivars. Using the $F_{ST}-\theta_{\pi}$ approach, we identified 13.08 Mb of putatively selected
357 regions covering 729 genes (Fig. 5a). Over a dozen regions were similarly selected in
358 two or three of the subgenomes (Fig. 5b). We also applied the XP-EHH and XP-CLR
359 methods, which led to the identification of a 2.68-Mb putatively selected region
360 (covering 951 genes) and a 26.08-Mb putatively selected region (covering 3,232

361 genes), respectively (Supplementary Table 9). Finally, we excluded the selected
362 regions identified in our earlier comparison of all cultivars and landraces to focus on
363 local adaptation. A total of 3,814 genes were identified using all three methods, with 51
364 genes being commonly detected (Fig. 5d and Supplementary Table 9e). Among the
365 regions commonly identified using all three approaches, we found that *TaPGIP1*, a
366 polygalacturonase-inhibiting defense protein⁴⁵; *WRKY27*, involved in disease
367 resistance⁴⁶; *TaNAK*, a putative protein kinase involved in defense⁴⁷; and *TaPHB2*, a
368 mitochondrial prohibitin complex protein⁴⁸, were all located within a selected region
369 on chromosome 2A (Fig. 5c). The regions on chromosomes 2B and 2D syntenic to
370 this region were also under selection. Another selected region on chromosome 3A
371 contains *TaPIN1*, required for auxin-dependent root branching⁴⁹; *TaPrx*, related to
372 oxidative stress⁵⁰; and *TaPEPRI*, involved in the innate immunity response⁵¹ (Fig.
373 5c). A detailed haplotype frequency analysis indicated that the frequencies of the
374 primary haplotypes in the European landraces were lower than in the Chinese
375 cultivars for all six genes (Fig. 5e and f).

376 The West Asian landraces are the most closely related modern relatives of the
377 ancestral wheat population. We therefore compared the European and Chinese
378 landraces to the West Asian landraces to identify the regions selected during local
379 adaptation as wheat gradually spread to the west and the east. Using $F_{ST}-\theta_{\pi}$, XP-EHH,
380 and XP-CLR analyses, we identified 22.75-Mb (covering 1,760 genes), 3.00-Mb
381 (covering 1,074 genes), and 21.04-Mb (covering 2,619 genes) putatively selected
382 regions between the European and West Asian landraces, respectively
383 (Supplementary Table 10). These selected regions overlap with a few reported QTLs,
384 including two associated with flour quality⁵². We identified a significantly selected
385 region on chromosome 2B that contains *TaNPF6.1-2B*, another ortholog of the
386 *Arabidopsis* nitrate transporter gene *NRT1.1* (Supplementary Fig. 12a). The same
387 region also harbors *TaFBP7*, a gene related to temperature response⁵³, and *TaANPI*,
388 an oxidative stress responsive gene⁵⁴. Whereas novel haplotypes for *TaNPF6.1-2B*

389 emerged in the European landraces, the genotypes typically maintained one of the two
390 *TaFBP7* and *TaANP1* haplotypes from the West Asian landraces (Supplementary Fig.
391 12b and c).

392 When comparing the Chinese landraces with the West Asian landraces, we
393 identified 8.94 Mb of putatively selected regions (covering 550 genes) using $F_{ST}-\theta_{\pi}$,
394 2.81 Mb (covering 1,027 genes) using XP-EHH, and 18.85 Mb (covering 2,392
395 genes) using XP-CLR (Supplementary Table 11). One of the genes identified in the
396 selected regions was *TaOSH43* (Supplementary Fig. 13a), which regulates shoot
397 meristem homeostasis and thus plant architecture and spike development⁵⁵. A new
398 haplotype emerged and became dominant in the Chinese landraces (Supplementary
399 Fig. 13b and c). We also found that a flour-quality QTL⁵² overlaps with a selected
400 region on chromosome 6B.

401

402 **Discussion**

403 Our analysis of 120 representative bread wheat accessions revealed a unique pattern
404 of genome changes that occurred during wheat adaption and modern breeding,
405 especially in China. The allopolyploidization of hexaploid bread wheat is expected to
406 have occurred under human cultivation, as bread wheat only exists in cultivated
407 forms^{3,10}. Consistent with this, bread wheat has a substantially lower genome diversity
408 than other crop and weed species (Fig. 1c and Table 1). Nevertheless, gene flow from
409 the allotetraploid *T. turgidum* (AABB) is likely to have contributed to the genetic
410 diversity of the A and B subgenomes in bread wheat^{27,28}, which means these two
411 subgenomes harbor more selective sweeps, as was demonstrated here. By contrast, the
412 barrier to gene flow from the diploid *Ae. tauschii* (DD) to bread wheat is much higher,
413 as suggested by the substantially lower nucleotide diversities in the D subgenome,
414 higher numbers of rare mutations, and fewer selective sweeps reported here.

415 Bread wheat has a long cultivation history and has been adapted to a wide
416 range of environmental conditions. The rich genetic diversity in cultivated accessions
417 and the lack of a wild bread wheat mean the gene flow among geographic regions is
418 potentially substantial. Indeed, we found that modern wheat breeding in China
419 significantly used the genetic diversity of the European landraces. In future breeding
420 programs, the genetic diversity of landraces from diverse geographic regions may
421 provide the additional genetic diversity required to fulfill the demands of our
422 increasing population and changing climate.

423 We found that different ancestors made distinct contributions to each
424 subgenome. In the Chinese cultivars, the genetic diversity of the A and B subgenomes
425 was mainly contributed by the European landraces. By contrast, the D subgenome of
426 the Chinese cultivars contains more diversity from local landraces. Although the
427 European landraces and the Chinese landraces have similar levels of genetic diversity
428 for each subgenome (Fig. 2d), the European landraces experienced continuous gene
429 exchange with the allotetraploid *T. turgidum*. Such a gene exchanges may diversify
430 favorable alleles that would be selected during modern breeding in China. On the
431 other hand, the D subgenome has limited genetic exchange in all landraces. As a
432 result, the D subgenome of the European landraces may not have additional
433 advantages over Chinese landraces as the A and B subgenomes have. These
434 differences may explain the different contribution of AB and D subgenomes to the
435 Chinese cultivars. Alternatively, the selection of accessions may lead to inevitable
436 bias, although we have used genome-wide markers to ensure that the resequenced
437 accessions represent the widest genome diversity.

438 We have narrowed down the selective sweeps corresponding to selection
439 during wheat diversification and modern breeding, which will be useful for the future
440 characterization of genes underlying important traits. Consistent with the
441 contributions of different ancestors to each subgenome, we found that the

442 homoeologous genes in the different subgenomes are often under differential
443 selection, suggesting that it may be feasible to target a single copy of a homoeologous
444 gene during breeding.

445

446 **Methods**

447 **Plant materials**

448 A total of 120 hexaploid wheat (*Triticum aestivum*) accessions from Asia, Europe,
449 and America were used in this study, including 95 landraces and 25 cultivars. Among
450 them were 60 accessions, including 42 landraces, and 18 elite varieties, from a
451 Chinese mini core collection, which is estimated to represent the majority of the
452 genomic diversity (~70%) of the 23,090 accessions in the Chinese national
453 collection^{16,56}. Based on genome-wide simple sequence repeat (SSR) data, these 60
454 accessions were estimated to represent the widest genome diversity of the mini core
455 collection. The rest of the accessions were selected following the sequencing of 326
456 accessions collected from major wheat cultivation sites using the genotyping-by-
457 sequencing (GBS) method⁵⁷. Based on the GBS results, the other 60 varieties were
458 selected for inclusion in the study, including 16 from West Asia, 12 from Central and
459 South Asia, 1 from Japan, 24 from Europe, and 7 from the Americas, which represent
460 the widest genome diversity. All the accessions were purified in multiple rounds of
461 single-seed descent to ensure their homozygosity.

462

463 **Library preparation for Illumina next-generation sequencing**

464 Approximately 1.5 µg genomic DNA was extracted from each sample using the
465 CTAB method and prepared in libraries for sequencing using a TruSeq Nano DNA
466 HT sample preparation kit (Illumina, USA) following the manufacturer's
467 recommendations. Briefly, the genomic DNA samples were fragmented by sonication
468 to a size of ~350 bp, then end-polished, A-tailed, and ligated with the full-length

469 adapters for Illumina sequencing with further PCR amplification. Index codes were
470 added facilitate the differentiation of sequences from each sample. The PCR products
471 were purified (AMPure XP bead system; Beckman Coulter, USA) and the libraries
472 were analyzed for their size distribution using an Agilent 2100 Bioanalyzer (Agilent
473 Technologies, USA) and quantified using real-time PCR.

474

475 **Genome sequencing and quality control**

476 The libraries were sequenced using the Illumina HiSeq X platform (Illumina). In total,
477 ~21,676 Tb of raw data were generated. To ensure reliable reads without artificial
478 bias, the low-quality paired reads ($\geq 10\%$ unidentified nucleotides (N); > 10
479 nucleotides aligned to the adaptor, allowing $\leq 10\%$ mismatches; $> 50\%$ bases with a
480 Phred quality less than 5) were removed. A total of 21,531 Tb (~179.4 Gb per
481 sample) high-quality genomic data was obtained.

482

483 **Read mapping and SNP calling**

484 The remaining high-quality paired-end reads were mapped to the bread wheat
485 reference genome (IWGSC RefSeq v1.0) using Burrows-Wheeler Aligner software
486 with the command 'mem -t 4 -k 32 -M'⁵⁸. To reduce mismatches generated by the
487 PCR amplification before sequencing, the duplicated reads were removed with the
488 help of SAMtools (v0.1.19)⁵⁹. After the alignment, SNP calling was performed on a
489 population scale using a Bayesian approach in SAMtools. The genotype likelihoods
490 were calculated from the reads of each individual at each genomic location, and the
491 allele frequencies were determined using a Bayesian approach. The 'mpileup'
492 command was used to identify SNPs using the parameters '-q 1 -C 50 -S -D -m 2 -F
493 0.002'. To exclude the SNP calling errors caused by incorrect mapping or InDels,
494 only the 70,172,660 high-quality filtered SNPs (depth ≥ 4 , maf ≥ 0.01 , miss ≤ 0.1)
495 were used in the subsequent analysis.

496

497 **Functional annotation of genetic variants**

498 The SNP annotation was performed using the published wheat genome⁹ and the
499 ANNOVAR package (v2013-05-20)⁶⁰. Based on the genome annotation, the SNPs
500 were categorized as being in exonic regions (overlapping with a coding exon),
501 intronic regions (overlapping with an intron), splicing sites (within 2 bp of a splicing
502 junction), upstream or downstream regions (within a 1-kb region upstream or
503 downstream of a transcription start or stop site, respectively), or intergenic regions.
504 The SNPs in the coding exons were further grouped into synonymous SNPs (do not
505 cause amino acid changes) or non-synonymous SNPs (cause amino acid changes).
506 The mutations causing stop gain and stop loss were also classified into this group. To
507 exclude genes with possible structural annotation errors, those expressed in the leaves
508 or existing in multiple copies were selected as HC genes for further analysis.

509

510 **Population genetic diversity**

511 Nucleotide diversity $\theta\pi$ and fixation index (F_{ST}) were calculated using VCFtools
512 (v0.1.14)⁶¹, while Watterson's estimator (θ_w) and Tajima's D were calculated using
513 VariScan (v2.0.3)⁶². These population statistics were analyzed using the sliding-
514 window approach (20-kb windows with 10-kb increments). HC genes were selected
515 to identify single-copy orthologous genes between the A, B, and D subgenomes using
516 Proteinortho (v5.16), with default settings⁶³.

517

518 **Linkage disequilibrium analysis**

519 To estimate and compare the patterns of linkage disequilibrium (LD) between
520 different populations, the squared correlation coefficient (r^2) between pairwise SNPs
521 was computed using the software Haploview (v4.2)⁶⁴. The program parameters were
522 set as '-n -dprime -minMAF 0.1'. The average r^2 value was calculated for pairwise
523 markers in a 500-kb window and averaged across the whole genome.

524

525 **Phylogenetic tree and population structure**

526 A total of 1,925,854 SNPs in coding regions (exonic and intronic) were used for the
527 population genetics analysis. To clarify the phylogenetic relationship from a genome-
528 wide perspective, an individual-based neighbor-joining tree was constructed using the
529 *p*-distance in the software TreeBeST (v1.9.2), with bootstrap values determined from
530 1000 replicates⁶⁵.

531 The population genetic structure was examined using the program
532 ADMIXTURE (v1.23)⁶⁶. First, 95 landraces were used to estimate the genetic
533 ancestry, specifying a *K* ranging from 2 to 8. The most suitable number of ancestral
534 populations was determined to be *K* = 3, for which the lowest cross-validation error of
535 0.492 was obtained. A principal component analysis (PCA) was also conducted to
536 evaluate the genetic structure of the populations using the software GCTA⁶⁷. First, a
537 genetic relationship matrix (GRM) was obtained using the parameter ‘–make-grm’,
538 then the top three principal components were estimated with the parameter ‘–pca3’.
539

540 **Population admixture analyses**

541 The population relatedness and migration events were inferred using TreeMix⁶⁸. A
542 total of 113 varieties with little admixture were selected to represent the seven
543 subgroups. The 1,925,854 coding-region SNPs were used to build a maximum
544 likelihood tree, using a window size of 2000 SNPs. This was repeated 10 times, using
545 the West Asian landraces as the root group. The tree with the lowest standard error for
546 the residuals was selected as the base tree topology. The population pairs with an
547 above zero standard residual error were identified as candidates for admixture events,
548 which represent populations which the data indicate are more closely related to each
549 other than is demonstrated in the best-fit tree⁶⁸. TreeMix was then run using between
550 one and six introduced migration events. When three migration events were added,
551 the residuals were much lower than for the trees generated using other numbers of
552 migration events.

553

554 **Introgression analysis**

555 The identity scores (IS) were calculated³² to visualize the shared haplotypes between
556 the three populations (European varieties, Chinese landraces, and Chinese cultivars).

557 The IS values were used to evaluate the similarities of every sequenced sample to the
558 reference genome (Chinese Spring) within 20-kb windows. The IS was calculated
559 using the following formula:

$$560 \quad IS = \frac{\sum_{i=1}^N |Ds_{1i} - Ds_{2i}|}{\text{number of SNPs in the window}}$$

561 where D represents genotype similarity to reference genome of samples in single site.
562 The IS of any single site was calculated as the difference in the D between two
563 samples. The average IS value was calculated for each population.

564 The H_P (population heterozygosity) was calculated for each candidate
565 introgression region. At each detected SNP position, the numbers of reads
566 corresponding to the most and least frequently observed allele (n_{MAJ} and n_{MIN} ,
567 respectively) were counted in each population. The H_P for each window was
568 calculated using the following formula:

$$569 \quad H_P = \frac{2 \sum n_{MAJ} \sum n_{MIN}}{(\sum n_{MAJ} + \sum n_{MIN})^2}$$

570 $\sum n_{MAJ}$ and $\sum n_{MIN}$ are sums of the n_{MAJ} and n_{MIN} values, respectively, calculated
571 for all SNPs in the 20-kb window (sliding in 10-kb steps)⁶⁹. The population
572 recombination rate was estimated from the SNPs of three populations (European
573 varieties, Chinese landraces, and Chinese cultivars) within a 20-kb window using the
574 R package FastEPRR (v1.0)⁷⁰.

575

576 **Genome-wide selective sweep analysis**

577 A sliding-window approach (20-kb windows sliding in 10-kb steps) was applied to
578 quantify the levels of polymorphism (θ_π , the pairwise nucleotide variation as a
579 measure of variability) and genetic differentiation (F_{ST}) between the different
580 populations using the VCFtools software (v0.1.14)⁶¹. The θ_π ratios were \log_2 -
581 transformed. Subsequently, the empirical percentiles of the F_{ST} and $\log_2(\theta_\pi$ ratio)
582 values in each window were estimated and ranked. The windows with the top 5% F_{ST}
583 and $\log_2(\theta_\pi$ ratio) values were considered simultaneously as candidate outliers under
584 strong selective sweeps. All outlier windows were assigned to corresponding regions

585 and genes. The cross-population extended haplotype homozygosity (XP-EHH)
586 statistic was estimated⁷¹ for the cultivar group and the landrace group, using the
587 landrace group as a contrast. The genetic map was assumed to be 0.18 cM/Mb for the
588 A and B subgenome, and 0.341 cM/Mb for the D subgenome. The XP-CLR score³⁵
589 was used to confirm the selective sweeps on the basis of domestication features, with
590 the highest being 1%, via the cross-population composite likelihood method.

591

592 **Candidate gene analysis**

593 Gene Ontology (GO) and Kyoto Encyclopedia of Genes and Genomes (KEGG)
594 analyses were performed on the candidate genes (all annotated genes in the outlier
595 windows denoted by the top 5% of the F_{ST} and $\log_2(\theta_\pi)$ ratio) values, the top 1% of the
596 XP-EHH values, and the top 1% of the XP-CLR scores). The candidate genes were
597 also attributed to known KEGG pathways (<http://www.kegg.jp>).

598

599 **PCR primers and amplicon sequence analysis**

600 A total of 28 Chinese cultivars developed between the 1940s and the 2000s were
601 analyzed to clarify the changes in the haplotypes of the candidate genes during wheat
602 breeding. All primers were designed using the Primer 5.0 software and listed in Table
603 S13a. DNAMAN8.0 was used to align the sequences to the reference genome and
604 identify the SNPs, after which the frequencies of the main haplotypes in the candidate
605 genes were analyzed.

606

607 **Data availability**

608 The sequencing data from this study have been deposited into the Sequence Read
609 Archive (<https://www.ncbi.nlm.nih.gov/sra>) under accession PRJNA439156.

610

611 **References**

- 612 1. Salamini, F., Ozkan, H., Brandolini, A., Schafer-Pregl, R. & Martin, W.
613 Genetics and geography of wild cereal domestication in the near east. *Nat Rev*
614 *Genet* **3**, 429-41 (2002).
- 615 2. Gornicki, P. *et al.* The chloroplast view of the evolution of polyploid wheat.
616 *New Phytol* **204**, 704-14 (2014).
- 617 3. Dubcovsky, J. & Dvorak, J. Genome plasticity a key factor in the success of
618 polyploid wheat under domestication. *Science* **316**, 1862-6 (2007).
- 619 4. International Wheat Genome Sequencing Consortium. A chromosome-based
620 draft sequence of the hexaploid bread wheat (*Triticum aestivum*) genome.
621 *Science* **345**, 1251788 (2014).
- 622 5. Marcussen, T. *et al.* Ancient hybridizations among the ancestral genomes of
623 bread wheat. *Science* **345**, 1250092 (2014).
- 624 6. Chapman, J.A. *et al.* A whole-genome shotgun approach for assembling and
625 anchoring the hexaploid bread wheat genome. *Genome Biol* **16**, 26 (2015).
- 626 7. Brenchley, R. *et al.* Analysis of the bread wheat genome using whole-genome
627 shotgun sequencing. *Nature* **491**, 705-10 (2012).
- 628 8. Clavijo, B.J. *et al.* An improved assembly and annotation of the allohexaploid
629 wheat genome identifies complete families of agronomic genes and provides
630 genomic evidence for chromosomal translocations. *Genome Res* **27**, 885-896
631 (2017).
- 632 9. International Wheat Genome Sequencing Consortium *et al.* Shifting the limits
633 in wheat research and breeding using a fully annotated reference genome.
634 *Science* **361**, eaar7191 (2018).
- 635 10. Feldmann, M. Origin of cultivated wheat. in *The world wheat book: a history*
636 *of wheat breeding.*, Vol. 1 (eds. Bonjean, A. & Angus, W.) 3-56 (Lavoisier
637 Publishing, Paris, France, 2001).
- 638 11. Zhou, Y. *et al.* Uncovering the dispersion history, adaptive evolution and
639 selection of wheat in China. *Plant Biotechnol J* **16**, 280-291 (2018).
- 640 12. Long, T. *et al.* The early history of wheat in China from (14)C dating and
641 Bayesian chronological modelling. *Nat Plants* **4**, 272-279 (2018).
- 642 13. He, Z.H., Rajaram, S., Xin, Z.Y. & Huang, G.Z. *A history of wheat breeding*
643 *in China*, (CIMMYT, Mexico, D. F., 2001).
- 644 14. Montenegro, J.D. *et al.* The pangenome of hexaploid bread wheat. *Plant J* **90**,
645 1007-1013 (2017).
- 646 15. Jordan, K.W. *et al.* A haplotype map of allohexaploid wheat reveals distinct
647 patterns of selection on homoeologous genomes. *Genome Biol* **16**, 48 (2015).
- 648 16. Hao, C. *et al.* Genetic diversity and construction of core collection in Chinese
649 wheat genetic resources. *Chinese Sci Bull* **53**, 1518-1526 (2008).
- 650 17. Li, H. A statistical framework for SNP calling, mutation discovery,
651 association mapping and population genetical parameter estimation from
652 sequencing data. *Bioinformatics* **27**, 2987-93 (2011).

- 653 18. Paterson, A.H. *et al.* The *Sorghum bicolor* genome and the diversification of
654 grasses. *Nature* **457**, 551-6 (2009).
- 655 19. McNally, K.L. *et al.* Genomewide SNP variation reveals relationships among
656 landraces and modern varieties of rice. *Proc Natl Acad Sci U S A* **106**, 12273-
657 8 (2009).
- 658 20. Valliyodan, B. *et al.* Landscape of genomic diversity and trait discovery in
659 soybean. *Sci Rep* **6**, 23598 (2016).
- 660 21. Clark, R.M. *et al.* Common sequence polymorphisms shaping genetic
661 diversity in *Arabidopsis thaliana*. *Science* **317**, 338-42 (2007).
- 662 22. Akhunov, E.D. *et al.* Nucleotide diversity maps reveal variation in diversity
663 among wheat genomes and chromosomes. *BMC Genomics* **11**, 702 (2010).
- 664 23. Haudry, A. *et al.* Grinding up wheat: a massive loss of nucleotide diversity
665 since domestication. *Mol Biol Evol* **24**, 1506-17 (2007).
- 666 24. Gore, M.A. *et al.* A first-generation haplotype map of maize. *Science* **326**,
667 1115-7 (2009).
- 668 25. Xu, X. *et al.* Resequencing 50 accessions of cultivated and wild rice yields
669 markers for identifying agronomically important genes. *Nat Biotechnol* **30**,
670 105-11 (2011).
- 671 26. Mace, E.S. *et al.* Whole-genome sequencing reveals untapped genetic
672 potential in Africa's indigenous cereal crop sorghum. *Nat Commun* **4**, 2320
673 (2013).
- 674 27. Dvorak, J., Akhunov, E.D., Akhunov, A.R., Deal, K.R. & Luo, M.C.
675 Molecular characterization of a diagnostic DNA marker for domesticated
676 tetraploid wheat provides evidence for gene flow from wild tetraploid wheat to
677 hexaploid wheat. *Mol Biol Evol* **23**, 1386-1396 (2006).
- 678 28. Zohary, D. & Brick, Z. *Triticum dicoccoides* in Israel: notes on its distribution,
679 ecology and natural hybridization. *Wheat Inform. Serv.* **13**, 6-8 (1961).
- 680 29. Huang, X. *et al.* Genome-wide association studies of 14 agronomic traits in
681 rice landraces. *Nat Genet* **42**, 961-7 (2010).
- 682 30. Hufford, M.B. *et al.* Comparative population genomics of maize
683 domestication and improvement. *Nat Genet* **44**, 808-11 (2012).
- 684 31. Hwang, E.Y. *et al.* A genome-wide association study of seed protein and oil
685 content in soybean. *BMC Genomics* **15**, 1 (2014).
- 686 32. Ai, H. *et al.* Adaptation and possible ancient interspecies introgression in pigs
687 identified by whole-genome sequencing. *Nat Genet* **47**, 217-25 (2015).
- 688 33. Devos, K.M., Dubcovsky, J., Dvorak, J., Chinoy, C.N. & Gale, M.D.
689 Structural evolution of wheat chromosomes 4A, 5A, and 7B and its impact on
690 recombination. *Theor Appl Genet* **91**, 282-8 (1995).
- 691 34. Sabeti, P.C. *et al.* Genome-wide detection and characterization of positive
692 selection in human populations. *Nature* **449**, 913-8 (2007).
- 693 35. Chen, H., Patterson, N. & Reich, D. Population differentiation as a test for
694 selective sweeps. *Genome Res* **20**, 393-402 (2010).

- 695 36. Li, F. *et al.* Genome-wide linkage mapping of yield-related traits in three
696 Chinese bread wheat populations using high-density SNP markers. *Theor Appl*
697 *Genet* **131**, 1903-1924 (2018).
- 698 37. Wang, Y.Y., Hsu, P.K. & Tsay, Y.F. Uptake, allocation and signaling of
699 nitrate. *Trends Plant Sci* **17**, 458-67 (2012).
- 700 38. Buchner, P. & Hawkesford, M.J. Complex phylogeny and gene expression
701 patterns of members of the NITRATE TRANSPORTER 1/PEPTIDE
702 TRANSPORTER family (NPF) in wheat. *J Exp Bot* **65**, 5697-710 (2014).
- 703 39. Fang, Y. *et al.* A stress-responsive NAC transcription factor SNAC3 confers
704 heat and drought tolerance through modulation of reactive oxygen species in
705 rice. *J Exp Bot* **66**, 6803-17 (2015).
- 706 40. Gray, J.A., Shalit-Kaneh, A., Chu, D.N., Hsu, P.Y. & Harmer, S.L. The
707 *REVEILLE* clock genes inhibit growth of juvenile and adult plants by control
708 of cell size. *Plant Physiol* **173**, 2308-2322 (2017).
- 709 41. Peterson, K.M. *et al.* *Arabidopsis* homeodomain-leucine zipper IV proteins
710 promote stomatal development and ectopically induce stomata beyond the
711 epidermis. *Development* **140**, 1924-35 (2013).
- 712 42. Campbell, J.L. *et al.* Cloning of new members of heat shock protein *HSP101*
713 gene family in wheat (*Triticum aestivum* (L.) Moench) inducible by heat,
714 dehydration, and ABA. *Biochim Biophys Acta* **1517**, 270-7 (2001).
- 715 43. Hu, H. *et al.* Characterization of transcription factor gene *SNAC2* conferring
716 cold and salt tolerance in rice. *Plant Mol Biol* **67**, 169-81 (2008).
- 717 44. Sun, T., Li, S. & Ren, H. OsFH15, a class I formin, interacts with
718 microfilaments and microtubules to regulate grain size via affecting cell
719 expansion in rice. *Sci Rep* **7**, 6538 (2017).
- 720 45. Ferrari, S., Galletti, R., Vairo, D., Cervone, F. & De Lorenzo, G. Antisense
721 expression of the *Arabidopsis thaliana* *AtPGIP1* gene reduces
722 polygalacturonase-inhibiting protein accumulation and enhances susceptibility
723 to *Botrytis cinerea*. *Mol Plant Microbe Interact* **19**, 931-6 (2006).
- 724 46. Mukhtar, M.S., Deslandes, L., Auriac, M.C., Marco, Y. & Somssich, I.E. The
725 *Arabidopsis* transcription factor WRKY27 influences wilt disease symptom
726 development caused by *Ralstonia solanacearum*. *Plant J* **56**, 935-47 (2008).
- 727 47. Xu, P. *et al.* A brassinosteroid-signaling kinase interacts with multiple
728 receptor-like kinases in *Arabidopsis*. *Mol Plant* **7**, 441-4 (2014).
- 729 48. Piechota, J. *et al.* Unraveling the functions of type II-prohibitins in
730 *Arabidopsis* mitochondria. *Plant Mol Biol* **88**, 249-67 (2015).
- 731 49. Talboys, P.J., Healey, J.R., Withers, P.J. & Jones, D.L. Phosphate depletion
732 modulates auxin transport in *Triticum aestivum* leading to altered root
733 branching. *J Exp Bot* **65**, 5023-32 (2014).
- 734 50. Liu, G. *et al.* Profiling of wheat class III peroxidase genes derived from
735 powdery mildew-attacked epidermis reveals distinct sequence-associated
736 expression patterns. *Mol Plant Microbe Interact* **18**, 730-41 (2005).

- 737 51. Lori, M. *et al.* Evolutionary divergence of the plant elicitor peptides (Peps)
738 and their receptors: interfamily incompatibility of perception but compatibility
739 of downstream signalling. *J Exp Bot* **66**, 5315-25 (2015).
- 740 52. Jin, H. *et al.* Genome-wide QTL mapping for wheat processing quality
741 parameters in a Gaocheng 8901/Zhoumai 16 recombinant inbred line
742 population. *Front Plant Sci* **7**, 1032 (2016).
- 743 53. Calderón-Villalobos, L.I., Nill, C., Marrocco, K., Kretsch, T. &
744 Schwechheimer, C. The evolutionarily conserved *Arabidopsis thaliana* F-box
745 protein AtFBP7 is required for efficient translation during temperature stress.
746 *Gene* **392**, 106-16 (2007).
- 747 54. Savatin, D.V. *et al.* The *Arabidopsis* NUCLEUS- AND PHRAGMOPLAST-
748 LOCALIZED KINASE1-related protein kinases are required for elicitor-
749 induced oxidative burst and immunity. *Plant Physiol* **165**, 1188-1202 (2014).
- 750 55. Morimoto, R., Nishioka, E., Murai, K. & Takumi, S. Functional conservation
751 of wheat orthologs of maize *rough sheath1* and *rough sheath2* genes. *Plant*
752 *Mol Biol* **69**, 273-85 (2009).
- 753 56. Hao, C., Wang, L., Ge, H., Dong, Y. & Zhang, X. Genetic diversity and
754 linkage disequilibrium in Chinese bread wheat (*Triticum aestivum* L.) revealed
755 by SSR markers. *PLoS ONE* **6**, e17279 (2011).
- 756 57. Poland, J.A., Brown, P.J., Sorrells, M.E. & Jannink, J.L. Development of
757 high-density genetic maps for barley and wheat using a novel two-enzyme
758 genotyping-by-sequencing approach. *PLoS ONE* **7**, e32253 (2012).
- 759 58. Li, H. & Durbin, R. Fast and accurate short read alignment with Burrows-
760 Wheeler transform. *Bioinformatics* **25**, 1754-60 (2009).
- 761 59. Li, H. *et al.* The Sequence Alignment/Map format and SAMtools.
762 *Bioinformatics* **25**, 2078-9 (2009).
- 763 60. Wang, K., Li, M. & Hakonarson, H. ANNOVAR: functional annotation of
764 genetic variants from high-throughput sequencing data. *Nucleic Acids Res* **38**,
765 e164 (2010).
- 766 61. Danecek, P. *et al.* The variant call format and VCFtools. *Bioinformatics* **27**,
767 2156-8 (2011).
- 768 62. Vilella, A.J., Blanco-Garcia, A., Hutter, S. & Rozas, J. VariScan: Analysis of
769 evolutionary patterns from large-scale DNA sequence polymorphism data.
770 *Bioinformatics* **21**, 2791-3 (2005).
- 771 63. Lechner, M. *et al.* Proteinortho: detection of (co-)orthologs in large-scale
772 analysis. *BMC Bioinformatics* **12**, 124 (2011).
- 773 64. Barrett, J.C., Fry, B., Maller, J. & Daly, M.J. Haploview: analysis and
774 visualization of LD and haplotype maps. *Bioinformatics* **21**, 263-5 (2005).
- 775 65. Vilella, A.J. *et al.* EnsemblCompara GeneTrees: Complete, duplication-aware
776 phylogenetic trees in vertebrates. *Genome Res* **19**, 327-35 (2009).
- 777 66. Alexander, D.H., Novembre, J. & Lange, K. Fast model-based estimation of
778 ancestry in unrelated individuals. *Genome Res* **19**, 1655-64 (2009).

- 779 67. Yang, J., Lee, S.H., Goddard, M.E. & Visscher, P.M. GCTA: a tool for
780 genome-wide complex trait analysis. *Am J Hum Genet* **88**, 76-82 (2011).
781 68. Pickrell, J.K. & Pritchard, J.K. Inference of population splits and mixtures
782 from genome-wide allele frequency data. *PLoS Genet* **8**, e1002967 (2012).
783 69. Rubin, C.J. *et al.* Whole-genome resequencing reveals loci under selection
784 during chicken domestication. *Nature* **464**, 587-91 (2010).
785 70. Gao, F., Ming, C., Hu, W. & Li, H. New software for the fast estimation of
786 population recombination rates (FastEPRR) in the genomic era. *G3* **6**, 1563-71
787 (2016).
788 71. Sabeti, P.C. *et al.* Genome-wide detection and characterization of positive
789 selection in human populations. *Nature* **449**, 913-918 (2007).

790

791 **Acknowledgments**

792 We thank Yalong Guo and Wenfeng Qian for their valuable suggestions. This
793 research was supported by the Chinese Academy of Sciences (CAS; grant no.
794 XDA08020105 to Y.J. and XDA08040108 to H.C.), the National Natural Science
795 Foundation of China (grant no. 31430010 to Y.J., 31871245 to Ying W, and
796 31770311 to C.T.), the National Program for Support of Top-Notch Young
797 Professionals (Y.J.), University of CAS (grant no. 110601M206 to Ying W.), the
798 Beijing NOVA Program (grant no. Z161100004916107 to Ying W.), the National
799 Transgenic Science and Technology Program (grant no. 2016ZX08010-002 to C.T.),
800 and the CAS Youth Innovation Promotion Association (grant no. 2017139 to C.T.).

801

802 **Author information**

803 These authors contributed equally: H. Chen, C. Jiao, Ying Wang, Yuange Wang.

804

805 **Affiliations**

806 *State Key Laboratory of Plant Genomics, Institute of Genetics and Developmental*
807 *Biology, Chinese Academy of Sciences, Beijing 100101, China*

808 Haofeng Chen, Yuange Wang, Caihuan Tian, Haopeng Yu, Jing Wang, Yuling Jiao

809 *Novogene Bioinformatics Institute, Beijing 100083, China*

810 Chengzhi Jiao, Wenkai Jiang, Hongfeng Lu

811 *College of Life Sciences, University of Chinese Academy of Sciences, Beijing 100049,*

812 *China*

813 Ying Wang, Fei Lu, Xiangdong Fu, Yongbiao Xue, Hongqing Ling, Yuling Jiao

814 *West China Biomedical Big Data Center, West China Hospital/West China School of*

815 *Medicine, and Medical Big Data Center, Sichuan University, Chengdu 610041, China*

816 Haopeng Yu

817 *Department of Crop Genomics and Bioinformatics, College of Agronomy and*

818 *Biotechnology, National Maize Improvement Center of China, China Agricultural*

819 *University, Beijing 100193, China*

820 Xiangfeng Wang

821 *State Key Laboratory of Plant Cell and Chromosome Engineering, Institute of*

822 *Genetics and Developmental Biology, Chinese Academy of Sciences, Beijing 100101,*

823 *China*

824 Fei Lu, Xiangdong Fu, Yongbiao Xue, Hongqing Ling

825

826 **Contributions**

827 Y.J., H.Lu and Ying W. conceived of and designed the study. C.J., Yuange W., H.Y.,

828 J.W., X.W., W.J., and H.Lu performed the analyses. C.J., H.Lu, Y.J., Ying W., W.J.,

829 and H.Ling interpreted the data. H.C. Yuange W., C.T., J.W. F.L., X.F., Y.X., H.Ling,

830 and Y.J. contributed to data collection. Y.J., C.J., and H.Lu wrote the manuscript with

831 input from all coauthors.

832

833 **Competing interests**

834 The authors declare no competing interests.

835

836 **Corresponding authors**

837 Correspondence to Yuling Jiao (yljiao@genetics.ac.cn) or Hongfeng Lu

838 (luhongfeng@novogene.cn).

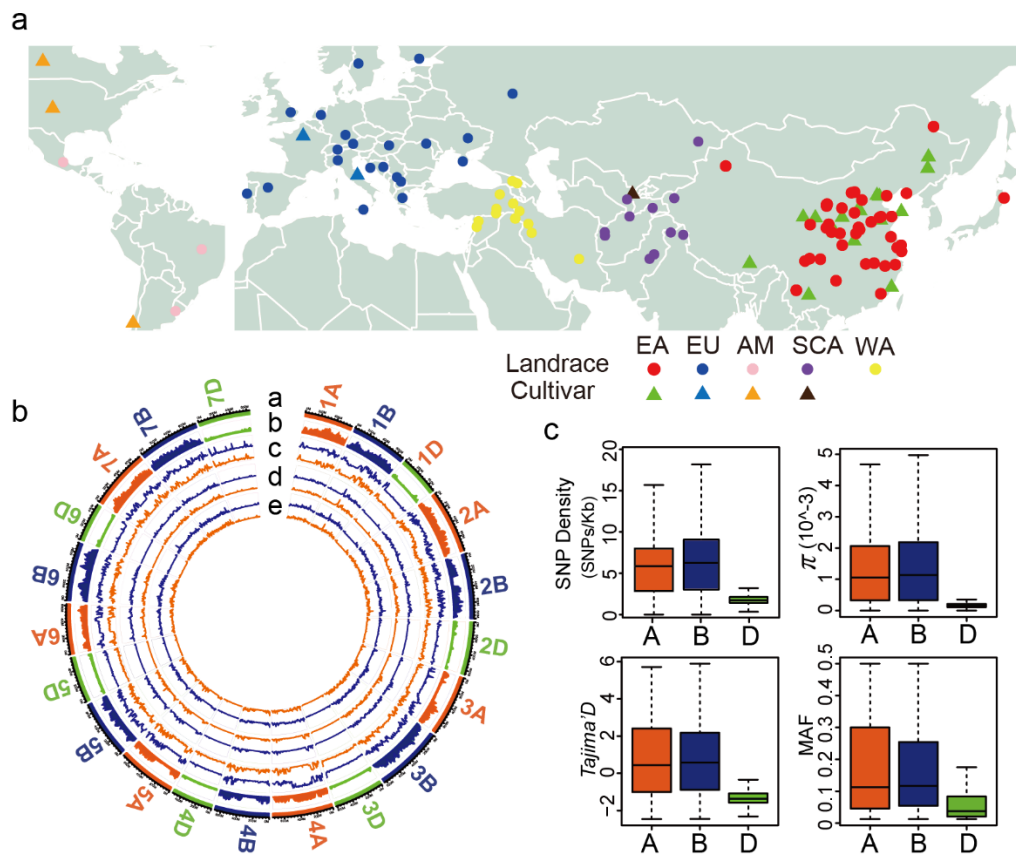
839

840 **Table**841 **Table 1.** Summary of the SNP distribution in the A, B, and D subgenomes.

Sub-genome	Up-stream ^a	Exonic						Intronic	3' UTR	5' UTR	5' UTR; 3' UTR ^b	Splicing	Down-stream ^c	Up/down Stream ^d	Intergenic
		Stop gain	Stop loss	Synonymous	Non-synonymous	N/S ratio	Unknowns								
A	325,784	8,180	1,782	133,267	207,728	1.56	27,325	366,052	11,108	12,388	1	1,466	302,952	46,595	27,276,394
B	349,547	9,130	1,953	141,373	224,779	1.59	30,931	394,269	11,557	14,315	11	1,615	324,819	52,059	31,395,654
D	124,077	3,487	644	82,817	105,693	1.28	8,690	151,873	5,590	5,881	4	660	117,057	18,823	7,287,737
Unknown	11,337	327	58	6,529	9,168	1.40	838	8,961	446	299	0	44	10,984	1,397	536,205
Total	810,745	21,124	4,437	363,986	547,368	1.50	67,784	921,155	28,701	32,883	16	3,785	755,812	118,874	66,495,990

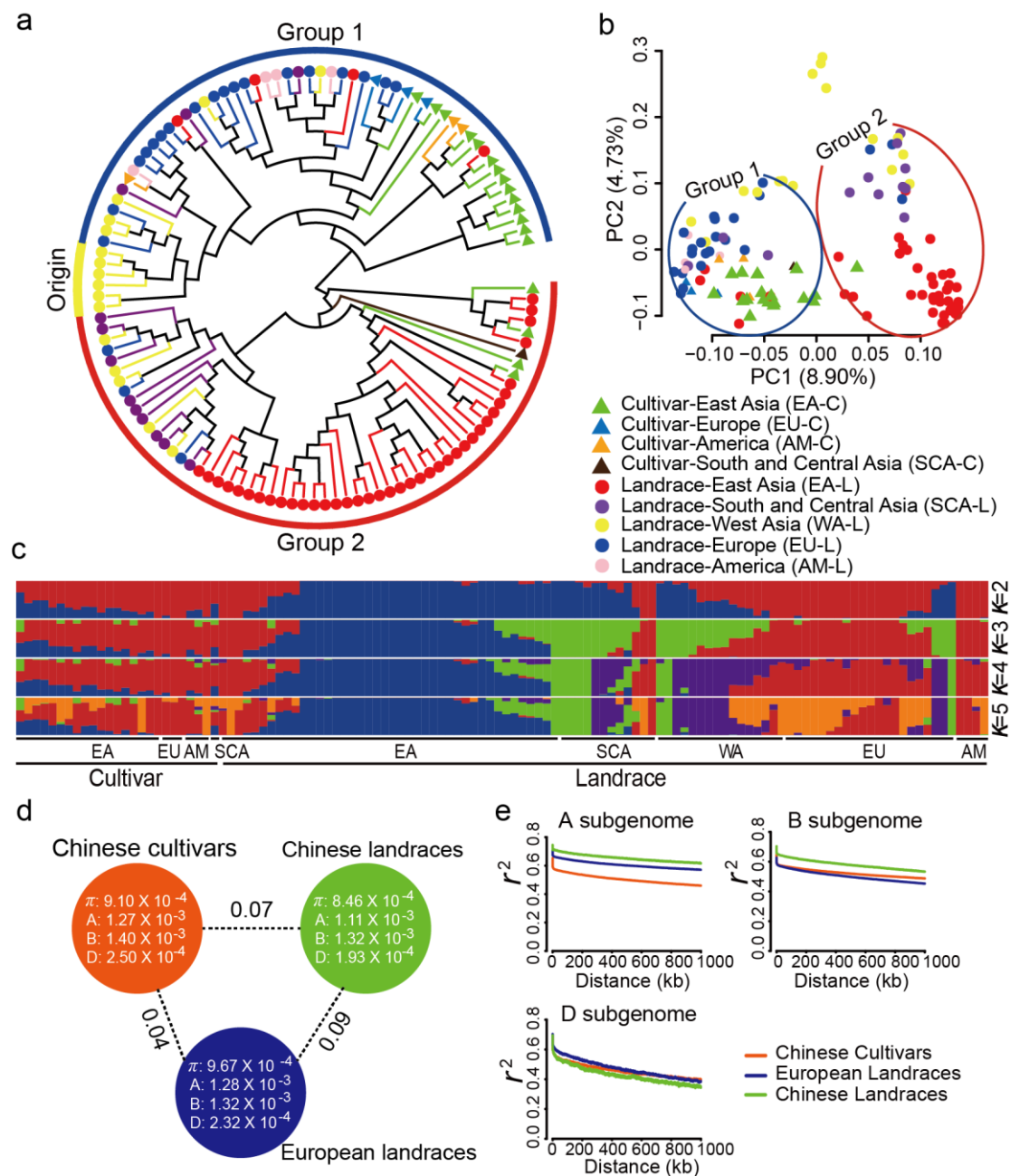
842 ^aRegions within the 1 kb before the start codon of the downstream gene.843 ^bRegions considered as both the 3'UTR of the upstream gene and 5'UTR of the downstream gene.844 ^cRegions within the 1 kb after the stop codon of the upstream gene.845 ^dRegions within the 1 kb after the stop codon of the upstream gene and also within the 1 kb before the start codon of the downstream gene.

846 **Figures**



847

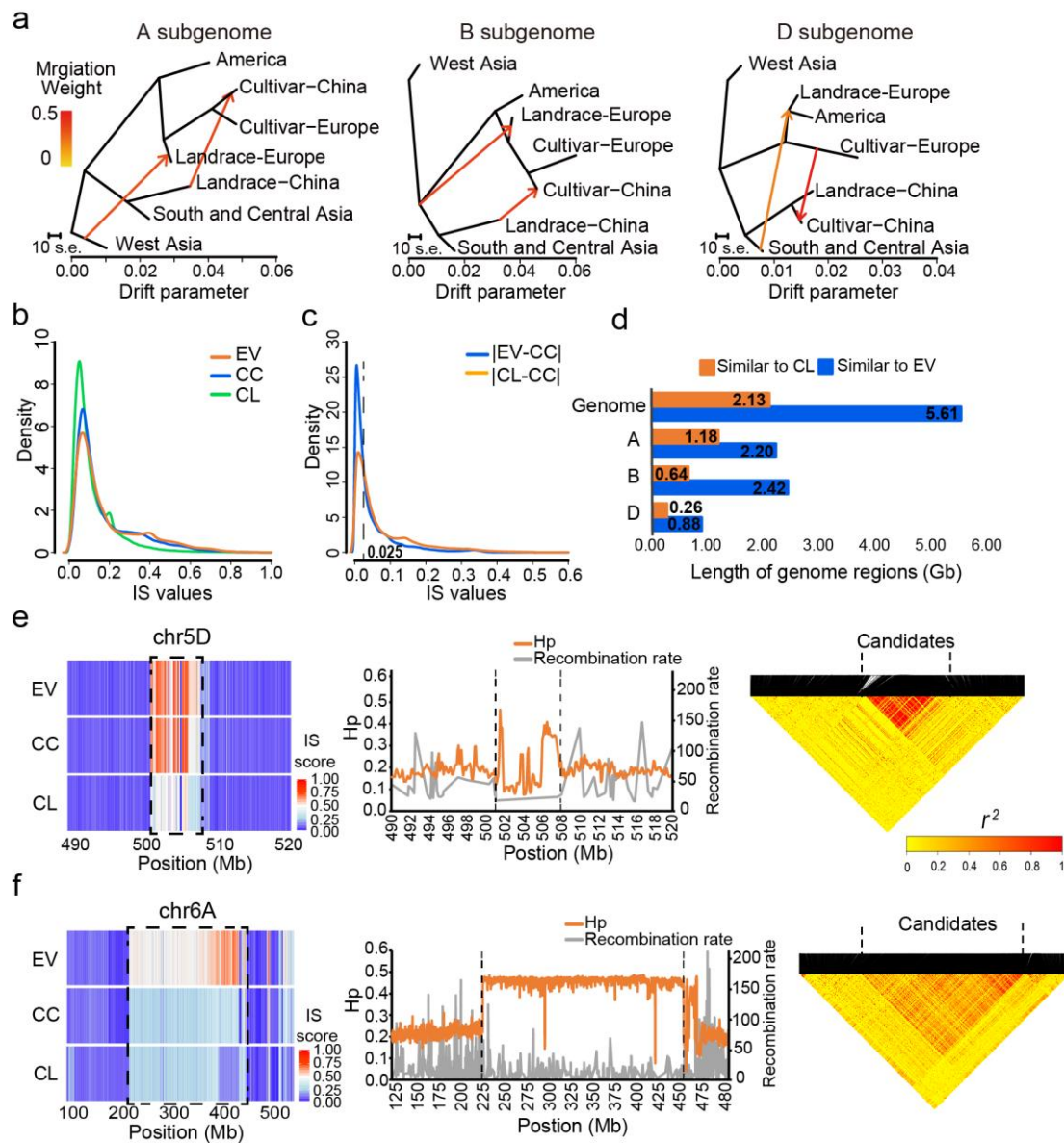
848 **Fig. 1.** Characterization of SNP distribution across the A, B, and D subgenome
849 chromosomes. (a) The geographic distribution of the 120 wheat accessions used in
850 this study. The circles represent landraces, while triangles represent cultivars.
851 Different colors represent populations from different geographic regions. EA, East
852 Asia; WA, West Asia; EU, Europe; AM, America; SCA, South and Central Asia. (b)
853 The genetic diversity of different populations along the chromosomes. From a to e,
854 the sections respectively represent the chromosomes, SNP density, neutral
855 evolutionary parameters (Tajima's D), nucleotide diversity parameters (θ_π), and
856 Watterson's θ , respectively. The red and blue lines in sections c to e represent the
857 cultivars and landraces, respectively. (c) Comparison of the genomic characteristics of
858 the A, B, and D subgenomes. MAF, minor allele frequencies.



859

860 **Fig. 2.** Population structure of the 120 wheat accessions. (a) Phylogenetic tree of the
 861 wheat accessions used in this study. The triangles represent wheat cultivars, while
 862 circles represent the landraces. The different colors represent populations from
 863 different geographic locations. “Origin” represents West Asia, which is considered the
 864 origin of bread wheat. “Group 1” represents the genotypes derived from the westward
 865 migration of bread wheat, including the European and American landraces, and the
 866 cultivars from Europe, America, and China. “Group 2” represents the groups derived
 867 from the eastward migration of bread wheat, including the South, Central, and East

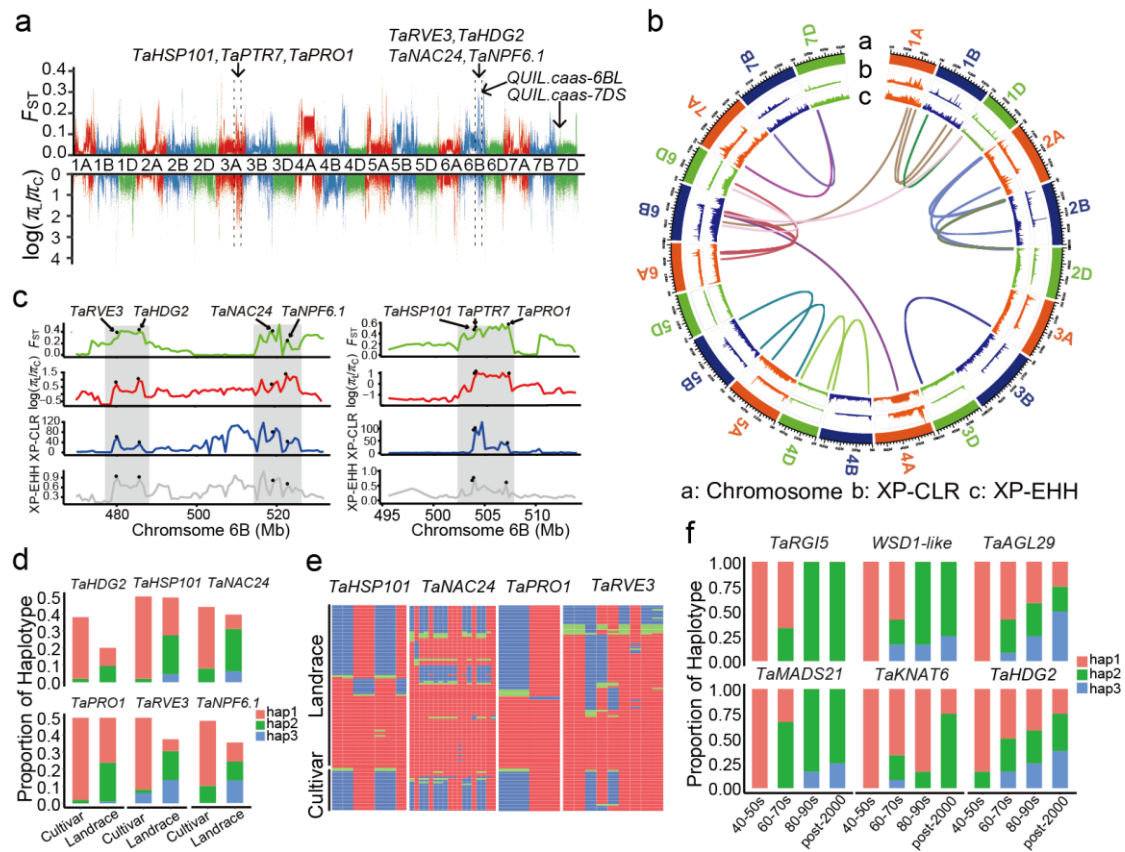
868 Asian landraces. **(b)** Principal component analysis of the 120 wheat accessions. **(a)**
869 and **(b)** share the same key. **(c)** Population structure of the 120 wheat accessions. **(d)**
870 Nucleotide diversity (π) and population divergence (F_{ST}) across the Chinese cultivars,
871 Chinese landraces, and European landraces. The values in each circle represent a
872 measure of nucleotide diversity for this group and each of its subgenomes, while the
873 values on each line indicate the population divergences between the two compared
874 groups. **(e)** Decay of linkage disequilibrium (LD) in the A, B, and D subgenomes of
875 three populations.



876

877 **Fig. 3.** Haplotype introgressions from the European and Chinese landraces into the
 878 Chinese cultivars. **(a)** Inferred phylogenetic trees of the A, B, and D subgenomes of
 879 different populations, including mixture events. Horizontal branch lengths are
 880 proportional to the amount of genetic drift. Migration arrows are colored according to
 881 their weight. **(b)** Density distribution of identity score (IS) values for three
 882 populations. **(c)** Density distribution of the difference in IS values between two
 883 populations. |EL-CC| represents the absolute value of the IS differences between the
 884 European varieties and the Chinese cultivars. |CL-CC| represents the absolute value of
 885 the IS differences between the Chinese landraces and the Chinese cultivars. **(d)**

886 Amount of similar genomic regions between populations. Orange represents the
887 length of similar genomic regions between the Chinese cultivars and the Chinese
888 landraces, and blue represents the length of similar genomic regions between the
889 Chinese cultivars and the European varieties. The statistical results of the entire
890 genome (Genome) as well as the individual A, B, and D subgenomes. The numbers
891 represent the total length of the similar genomic regions (Gb). (e) Candidate
892 introgression region between the European varieties and the Chinese cultivars. The
893 left panel presents details of the 8-Mb candidate region, located on chromosome 5D,
894 in which the Chinese cultivars are more similar to the European varieties than the
895 Chinese landraces. The middle panel represents the distribution of the population
896 heterozygosity (H_P) and recombination rates in this candidate region. The right panel
897 represents the LD heatmap of this candidate region. (f) Candidate introgression region
898 (200 Mb, located on chromosome 6A) between the Chinese landraces and Chinese
899 cultivars. The central and right panels are as described for (e).



900

901 **Fig. 4.** Population sweep selection during modern breeding between the cultivars and

902 landraces. (a) The distribution of the F_{ST} and θ_{π} ratio (landrace/cultivar) along the

903 chromosomes. The genome-wide threshold was defined by the top 5% of the F_{ST} and

904 θ_{π} ratio (landrace/cultivar) values. Candidate genes and QTLs were marked on the

905 map. (b) The distribution of XP-CLR and XP-EHH scores along the chromosomes.

906 From the outside to the inside, the data presented are the XP-CLR score, XP-EHH

907 score, and the duplicated copies of the homoeologous genes in the different

908 subgenomes under selection for every chromosome. (c) Seven genes distributed in

909 three candidate regions were commonly found to be under selection using the F_{ST} , θ_{π}

910 ratio, XP-CLR, and XP-EHH methods. The black points indicate the location of the

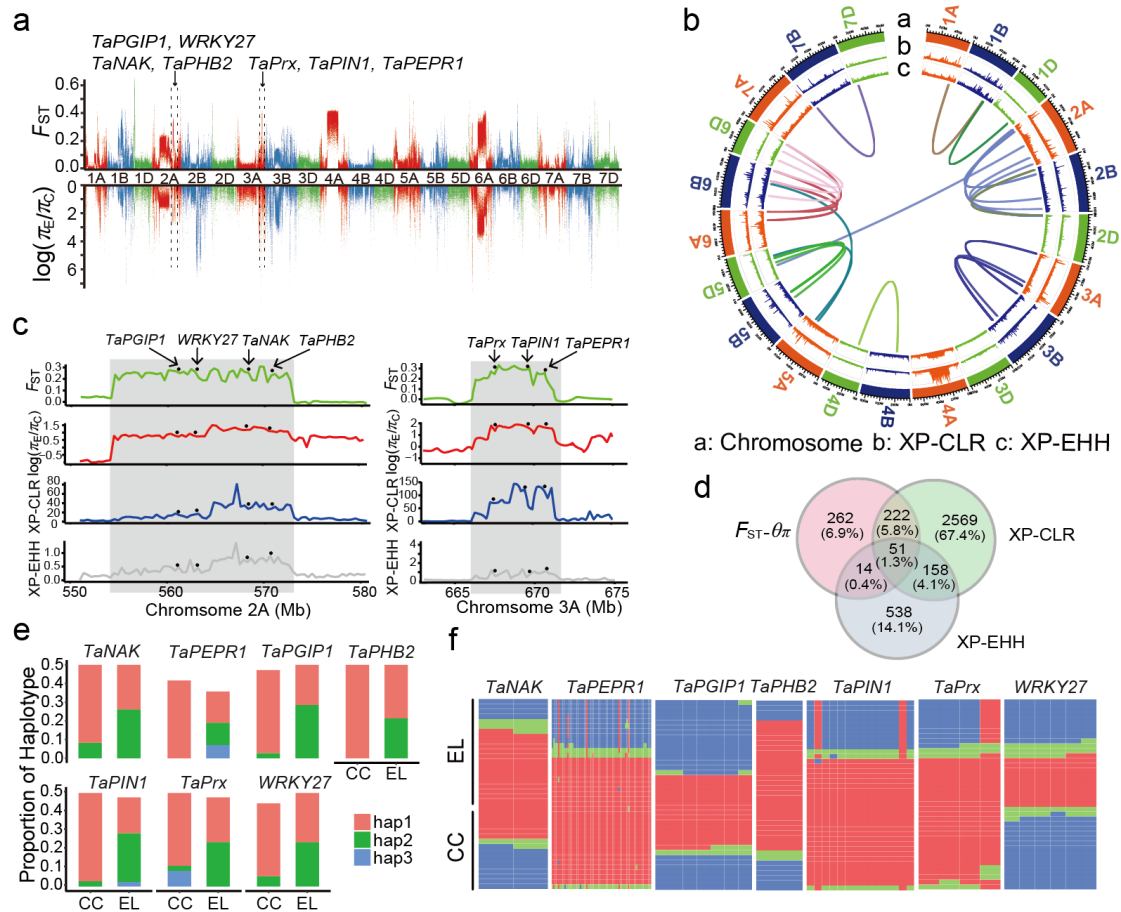
911 candidate selected genes on the chromosomes. (d) The haplotype frequency of the

912 candidate genes between the Chinese landrace and cultivar populations. (e) Heatmap

913 of genotypes in the putative selective sweeps. (f) The selection of the favored

914 haplotype frequencies in modern Chinese cultivars during wheat breeding since the

915 1940s.



916

917

Fig. 5. Population sweep selection during local adaptation in Chinese cultivars and

918

European landraces. **(a)** The distribution of the F_{ST} and θ_π ratio (European

919

landrace/Chinese cultivar) along the chromosomes. The genome-wide threshold was

920

defined by the top 5% of the F_{ST} and θ_π ratio (European landrace/Chinese cultivar)

921

values. Candidate genes and QTLs are marked on the map. **(b)** The distribution of

922

XP-CLR and XP-EHH scores along the chromosomes. From the outside to the inside,

923

the data presented are the XP-CLR score, the XP-EHH score, and the duplicated

924

copies of the homoeologous genes in the different subgenomes under selection along

925

every chromosome. **(c)** Seven genes distributed in the two candidate selection regions

926

identified using the $F_{ST}-\theta_\pi$ ratio, XP-CLR, and XP-EHH methods. The black points

927

indicate the location of the candidate genes on the chromosome; every gene has a

928

strong selection signal. **(d)** A Venn diagram of wheat genes under selection detected

929

using the $F_{ST}-\theta_\pi$ ratio, XP-CLR, and XP-EHH methods. **(e)** The haplotype frequency

930 of the candidate genes between the Chinese cultivars (CC) and the European
931 landraces (EL). **(f)** Heatmap of genotypes in the putative selective sweep.